In Situ Observation of Charge Exchange and Surface Segregation of Hydrogen during Low Energy H^+ and $H_2{}^+$ Scattering from Semiconductor Surfaces

R. Souda, E. Asari, T. Suzuki, T. Tanaka, and T. Aizawa
National Institute for Research in Inorganic Materials, 1-1 Namiki, Tsukuba, Ibaraki 305, Japan

(Received 22 December 1997)

The charge-exchange and diffusion/segregation dynamics of hydrogen has been investigated for Si(111), β-B(100), and $YB_{66}(100)$ surfaces. The backscattered proton yield during $H_2{}^+$ ion bombardment of the surfaces increases significantly with the irradiation time. This increase occurs because (i) the implanted hydrogen tends to segregate to the outermost surface layer and then passivates the active dangling bonds and (ii) energetic protons backscattered from the solid preferentially capture the dangling-bond electrons via transient chemisorption just before the protons leave the surface. [S0031-9007(98)06529-6]

PACS numbers: 79.20.Rf, 34.50.Fa, 34.70.+e

The dynamics of particle-solid interactions has recently attracted considerable attention. The fastest process, electron transition, occurs within an ultrashort time scale, in the femtosecond range. Understanding this process is a crucial prerequisite in the development of surface analysis techniques that use ions and should provide insight into surface chemistry such as molecular dissociation at surfaces [1,2]. Among various projectiles, the proton is the simplest elementary particle and plays an important role not only in surface chemistry but also in electrode reactions, plasma physics and thin-film growth, etc. [3–5]. However, very little is known about proton's dynamical properties, such as charge transfer, energy dissipation, screening, and making and breaking bonds during scattering. Moreover, hydrogen is a common impurity in many semiconductors and significantly affects their electronic properties by passivating defects and dopants. To date, although many studies have been done in this field [6–11], most of them involved the static behavior of hydrogen in bulk semiconductors. Diffusion/segregation dynamics of hydrogen is still poorly understood, evidenced by the large scatter in the reported values of the diffusion constant of hydrogen in bulk semiconductors [6]. This scatter is probably due to the complexity of the experimental techniques used. In this Letter, we therefore develop a more straightforward technique of scattering/implantation of hydrogen ions to gain more insight into such hydrogen dynamics.

Here, we report simultaneous observations of charge exchange and surface segregation of hydrogen on some covalent semiconductor surfaces. We found that the backscattered proton yield from Si(111) is significantly increased during H^+ and $H_2{}^+$ ($E_0 = 1$ keV) ion bombardment. This increase occurs because (i) implanted hydrogen segregates to the outermost surface layer after being thermalized, and then passivates the active dangling bonds and (ii) neutralization of energetic protons backscattered from the solid is suppressed by this passivation of the dangling bonds since a proton preferentially captures a dangling-bond electron via transient chemisorption just before leaving the surface. Thus, charge exchange of hydrogen even in the keV regime is intimately related to static chemisorption. Based on these findings, we develop a technique for *in situ* observation of hydrogen diffusion and hydrogen trapping by, e.g., bulk defects during $H_2{}^+$ ion bombardment. We then demonstrate the general applicability of this technique by using it to study hydrogen diffusion in well-defined surfaces of Si(111), $YB_{66}(100)$, β-B(100), and highly oriented pyrolytic graphite (HOPG).

The experiments were carried out in an ultrahigh vacuum (UHV) chamber (base pressure 2×10^{-10} mbar) equipped with facilities for standard surface characterization. The ion beams were extracted from the discharge of a He/H_2 gas mixture and then their mass analyzed by using a Wien filter (working pressure in the 10^{-10}-mbar range). The ions with kinetic energy of 1 keV were directed onto a surface at an incidence angle of 80° (with respect to the surface), and the ions backscattered through 160° were detected and energy analyzed using an electrostatic analyzer operating with a constant energy resolution of 2 eV. The ion-beam current was measured by using a Faraday cup so that the scattered ion yields were normalized relative to each other. The scattered ion yields were compared under the same experimental conditions by mounting two samples on a tandem sample holder. The Si(111) surface (undoped, 1000 Ω cm) was cleaned by resistive heating to 1500 K in UHV. The surface temperature was controlled by passing a current through the sample. The β-B(100) and $YB_{66}(100)$ surfaces were cut from the single crystal rods that were grown by a floating zone method [12], and then heated in the UHV chamber by electron bombardment from behind. The surface cleanliness was verified *in situ* by using He^+ ion scattering, time-of-flight ion-mass spectrometry (TOF-IMS), and low-energy electron diffraction (LEED).

Figures 1(a) and 1(b) show representative energy spectra of positive ions ejected from the Si(111) surface by the bombardment of incident 1-keV H^+ and $H_2{}^+$ beams,

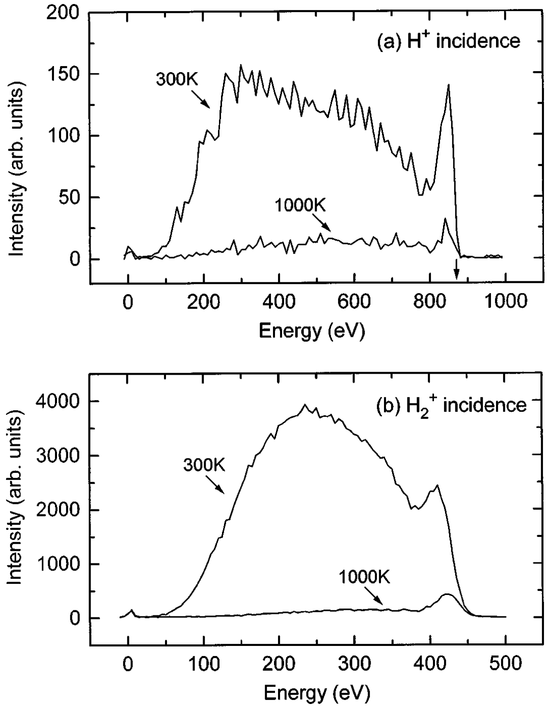

FIG. 1. Representative energy spectra of positive ions scattered from a Si(111) (7 × 7) surface by bombardment of an incident (a) 1-keV H^+ and (b) 1-keV $H_2{}^+$ beam. Scattering and incidence angles were 160° and 80°, respectively. Measurements were made at 300 and 1000 K. The arrow on the abscissa indicates the energy corresponding to elastic binary collision.

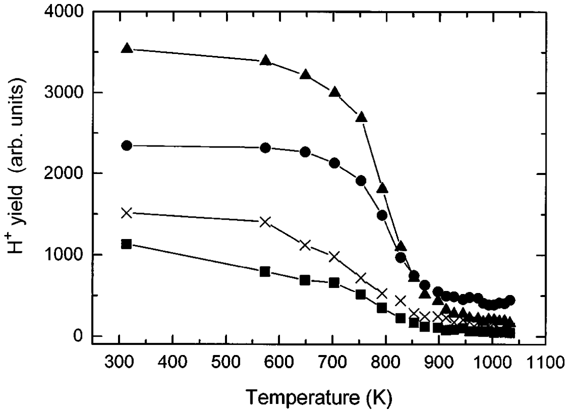

FIG. 2. Surface temperature dependence of the intensity of H^+ ions scattered from the Si(111) surface by a 1-keV $H_2{}^+$ beam for various energy levels (100, 300, and 410 eV are indicated with triangles, squares, and circles, respectively). For comparison, the intensity of sputtered secondary H^+ ions obtained from TOF-IMS measurements using a 1-keV He^+ beam is also shown (crosses).

respectively. The arrow on the abscissa indicates the energy corresponding to elastic binary collision (EBC). The $H_2{}^+$ ions are completely dissociated during the collision, and the spectrum is essentially identical to that obtained for a $E_0 = 500$-eV H^+ beam. The intensity of the energy spectrum taken at 300 K is significantly higher than that at 1000 K for both primary ions, and there is a pronounced broad peak extending from the EBC position towards the lower energy side. This broad spectral background is due to the multiple scattering of the H^+ ions that penetrate the outermost surface layer.

Figure 2 shows the temperature dependence of the scattered H^+ yield from the Si(111) surface obtained with incidence of the 1-keV $H_2{}^+$ beam. (For comparison, each yield was normalized by the ion beam current.) The ion yield decreases dramatically at around 800 K, which corresponds to the desorption temperature of chemisorbed hydrogen on the surface. Our TOF-IMS measurements (1-keV He^+ bombardment) reveal that H^+ ions are major secondary ions from the Si(111) surface after the $H_2{}^+$ irradiation. The temperature dependence of the sputtered secondary H^+ yield (crosses in Fig. 2) is similar to that of the scattered primary H^+ yield. These results strongly suggest that hydrogen implanted in a solid can readily segregate to the surface. The hydrogenated Si(111) surface still exhibited a sharp 7 × 7 pattern in LEED, showing that the surface damage induced by the $H_2{}^+$ beam is negligible.

The spectral feature of the H^+ ions scattered from the prehydrogenated Si(111) surface prepared by adsorption of atomic hydrogen was essentially identical to that from the $H_2{}^+$ (H^+) implanted Si(111) surface [13]. To gain more insight into the origin of the broadly humped background, we measured the TOF-IMS spectra during the $H_2{}^+$ ($D_2{}^+$) bombardment of the deuterated (hydrogenated) Si(111) surface. It is found that the spectral background comes only from the scattered primary ions and that no sputtered or recoiled chemisorbed hydrogen is involved [13,14].

The ions due to multiple scattering have a higher probability of neutralization relative to the ions due to single scattering from the topmost layer atom. However, this is not necessarily true for hydrogenated surfaces. The charge state of hydrogen in bulk Si may offer insight into the origin of such a spectral background. It has been suggested that a ground state of hydrogen in Si, which occupies a tetrahedral interstitial site, is in resonance with the valence band [6]; as hydrogen moves from this position, the resonance level shifts into the gap, thus forming a donor and acceptor level. This shift indicates that hydrogen in Si is electronically active. Indeed, the presence of H^+ has been assumed in p-type Si, which is responsible for rapidly drifting hydrogen species in an electric field. Such a free hydrogen (proton) is much less stable than bound hydrogen and tends to terminate an available dangling bond. In extraction of such a proton into the vacuum, the surface effect should play an important role. A proton should preferentially accommodate an electron of the active dangling bond of the clean Si(111) surface during formation of a transient chemisorption bond [15]. On the other hand, if the dangling bond is passivated by hydrogen, the 1s orbital of a backscattered proton tends to be nonbonding, thereby decreasing the electron capture probability at the passivated surface.

The charge state of such a static hydrogen might be related to the final charge fraction of scattered hydrogen. However, a very efficient positive ionization channel opens for energetic hydrogen during a violent collision with the surface atoms. Such a reionization process occurs in the asymmetric H-Si collision because the H 1s orbital has a strong antibonding character within a critical approach distance of 1.5 a.u. [15]. This distance is attained by hydrogen whose kinetic energy exceeds 25 eV, which is similar to the experimental threshold energy (~30 eV) at which the spectral background commences (Fig. 1). On the other hand, the symmetric H-H collision, where the H 1s orbital equally has both bonding and antibonding molecular-orbital character, does not lead to reionization [13]. This is also responsible for the absence of sputtered or recoiled H^+ ions during the H^+ ($H_2{}^+$) ion bombardment. Energetic H^+ ions are thus formed by reionization of hydrogen during asymmetric diatomic collisions with Si. The resulting H^+ ions undergo neutralization during transient chemisorption just before leaving the surface.

The proportionality between scattered proton yield and the coverage of hydrogen passivating the surface makes it possible to investigate the surface segregation of implanted hydrogen in real time. Figure 3 shows the dependence of the intensities of backscattered protons from the surfaces of Si(111), YB_{66}(100), β-B(100), and HOPG on bombardment time using the 1-keV $H_2{}^+$ beam. All measurements were done at room temperature at an $H_2{}^+$ flux of $(5.0 \pm 1.0) \times 10^{13}$ hydrogen ions $s^{-1}\,cm^{-2}$. For the Si(111) surface, the proton yield increases rapidly at the onset of bombardment. When the Si(111) surface is irradiated beforehand by the 1-keV He^+ beam, the increase in proton yield with time is gradual. The surface exhibited a 7 × 7 pattern in LEED even after the measurements. The increase in the proton yield is also gradual for the YB_{66}(100) and β-B(100) surfaces during the $H_2{}^+$ beam irradiation. For the HOPG surface, on the other hand, the yield slightly decreases with irradiation time. Table I lists the range and straggling of the implanted ions distribution as well as the damage formation calculated using a TRIM computer code.

For bulk Si, the reported values of the diffusion constant of hydrogen are highly scattered from 10^{-6} to 10^{-15} $cm^2\,s^{-1}$ [6]. At least three states of hydrogen are present in the equilibrium condition: (i) bound hydrogen at a dangling bond of a defect site, (ii) atomic hydrogen that occupies the interstitial site, and (iii) molecular hydrogen. The unbonded atomic hydrogen should be the most rapid diffuser in a crystalline Si. The steep increase in the proton yield at the onset of the $H_2{}^+$ irradiation of the Si(111) surface [Fig. 3(a)] arises from the passivation of the surface dangling bonds by segregated atomic hydrogen. The good agreement between the amount of implanted hydrogen within 10 s [$(5.0 \pm 1.0) \times 10^{14}$ cm^{-2}] and the density of the surface dangling bonds (3.04×10^{14} cm^{-2}) supports this supposition. It is thus found that most of the implanted hydrogen is segregated at the surface during this period and that the trapping of hydrogen in the bulk leading to the formation of defects or H_2 molecules is negligible during this onset period. This is not due to the temporal effect but to the ion-dosage effect, which we confirmed from several measurements using different ion beam intensities. Trapping of hydrogen by bulk defects is responsible for the suppressed increase in the scattered proton yield. This trapping is clearly seen in Fig. 3(a) when the surface is prebombarded by 1-keV He^+, which induces the bulk defects much more efficiently than does the 1-keV $H_2{}^+$ beam.

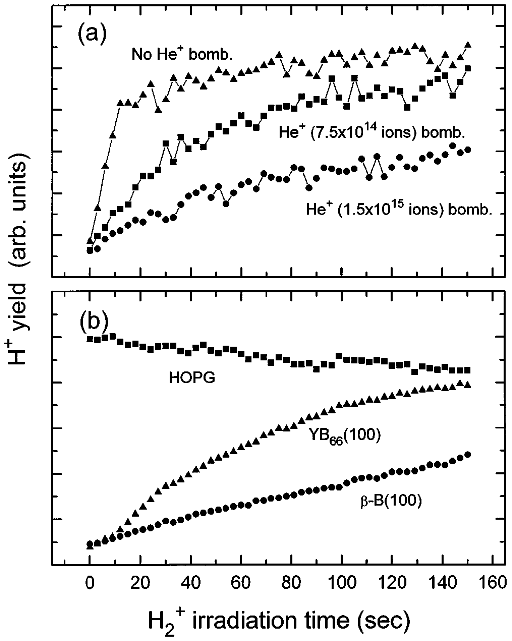

FIG. 3. Irradiation time dependence of the scattered proton yield using a 1-keV $H_2{}^+$ beam for (a) the Si(111) surface with and without prebombardment by 1-keV He^+ ions and (b) the YB_{66}(100), β-B(100), and HOPG surfaces without prebombardment. Measurements were made at room temperature at an $H_2{}^+$ flux of $(5.0 \pm 1.0) \times 10^{13}$ hydrogen ions $s^{-1}\,cm^{-2}$.

TABLE I. Range and straggling of the implanted primary ions (1-keV He^+ and $H_2{}^+$ beams) distribution in Si, B, and graphite, and the number of vacancies and sputtered target atoms per primary ion.

	$H_2{}^+$/Si	He^+/Si	$H_2{}^+$/B	$H_2{}^+$/C
Range (Å)	141	167	79	81
Straggling (Å)	76	94	30	32
Vacancies/ion	0.7	13.4	0.9	0.9
Sputtering yield	0.011	0.166	0.009	0.009

For both the β-B(100) and YB$_{66}$(100) surfaces, the lattice is formed by the covalently bonded B network consisting of an electron-deficient icosahedron. Termination of the surface by B$_{12}$ clusters was confirmed by the scanning tunneling microscopy image of YB$_{66}$(100) [16]. The segregation of implanted hydrogen in β-B and YB$_{66}$ is rather slow compared with that in Si despite the fact that the depth range of implanted hydrogen in B is shallower than that in Si, indicating that hydrogen is trapped more efficiently in bulk B. The neutral icosahedron has an affinity for two additional electrons so that hydrogen can be trapped in the lattice, causing the hydrogen to donate an electron. Also possible is the formation of three-centered bonds,

H
/ \
B—B ,

which is characteristic of boron hydrate. The slower increase in the proton yield for β-B than that for YB$_{66}$ [Fig. 3(b)] may be related to the lack of yttrium, which acts as an electron donor in the YB$_{66}$. The different behavior of the proton yield with irradiation time for HOPG can be explained by the efficient trapping of the implanted hydrogen in the bulk interstitial site and by the extremely unstable chemisorption state of hydrogen on the surface. Moreover, the large proton yield from HOPG may arise from the relatively inefficient hybridization of the H 1s orbital with the π orbital of HOPG during the transient chemisorption. The gradual decrease in the proton yield with irradiation time is related to the formation of point defects (or broken bonds) on the surface from which a proton captures an electron more efficiently.

As regards neutralization, it is currently held that protons do not form a bound electron state in solids but are screened by conduction electrons [17]. If a proton is screened, the scattered ion fraction is proportional to $E\omega_p^{-2/3}$, where E is the ion energy and ω_p is the plasma frequency. As seen in Fig. 3, however, the H$^+$ yield from the semiconductors is much smaller than from HOPG, which is apparently incompatible with this conventional picture since the plasma frequency of HOPG is much larger than that of the semiconductors. Moreover, the validity of the molecular orbital picture requires the existence of a bound electron state [15,18]. Note that the proposed mechanism of reionization is essentially identical to secondary ion formation [19]. For elemental surfaces, the fraction of secondary ions during the sputtering process is very small but is enhanced by several orders of magnitude if the surface undergoes chemical reaction with electronegative species such as oxygen. Similarly, there is a remarkable increase in the scattered H$^+$ (D$^+$) yield on a metal (Ta) and a semiconductor (Si) surface after oxygenation [20]. If the impinging proton is neutralized at the surface, the situation is exactly the same as sputtering of secondary ions. In both cases, therefore, a positive ion is formed due to reionization during asymmetric collision with chemisorbed oxygen, after which the partly ionic bonds are broken.

In summary, we have investigated the dynamics of the fastest electronic transition (10^{-15} s) and the slowest diffusion/segregation ($\sim$1 s) of hydrogen. We found that the dynamical charge transfer even in the keV regime is intimately related to a static chemisorption process, which also bridges the charge states of the hydrogen in the bulk and the hydrogen ejected into the vacuum. These findings demonstrate the potential of this technique for *in situ* observation of hydrogen diffusion in bulk semiconductors.

[1] P. Haochang *et al.*, Phys. Rev. Lett. **57**, 3035 (1986).
[2] B. Willerding *et al.*, Nucl. Instrum. Methods Phys. Res., Sect. B **13**, 614 (1986).
[3] C. T. Rettner *et al.*, Phys. Rev. Lett. **69**, 383 (1992).
[4] C. Astaldi *et al.*, Phys. Rev. Lett. **68**, 90 (1992).
[5] K. Sumitomo *et al.*, Phys. Rev. Lett. **66**, 1193 (1991).
[6] S. J. Pearton, J. W. Corbett, and T. S. Shi, Appl. Phys. A **43**, 153 (1987), and references therein.
[7] N. M. Johnson, C. Herring, and D. J. Chadi, Phys. Rev. Lett. **56**, 769 (1986).
[8] C. G. Van de Walle, Y. Bar-Yam, and S. T. Pantelides, Phys. Rev. Lett. **60**, 2761 (1988).
[9] K. J. Chang and D. J. Chadi, Phys. Rev. Lett. **62**, 937 (1989).
[10] K. Murakami *et al.*, Phys. Rev. Lett. **77**, 3161 (1996).
[11] N. M. Johnson *et al.*, Phys. Rev. B **35**, 4166 (1987).
[12] T. Tanaka, S. Otani, and Y. Ishizawa, J. Cryst. Growth **99**, 994 (1990).
[13] R. Souda *et al.* (to be published).
[14] The TRIM simulation also shows that the yield of sputtered/recoiled secondary hydrogen ions, if any, peaks at an energy well below 100 eV. The small peak appearing around the zero energy position in Fig. 1 is an artifact coming from the analyzer, confirmed by applying the bias voltage to the sample.
[15] R. Souda *et al.*, Phys. Rev. B **50**, 18 489 (1994).
[16] C. L. Perkins *et al.*, Phys. Rev. Lett. **77**, 4772 (1996).
[17] M. Kleber and J. Zwiegel, Phys. Rev. A **19**, 579 (1979).
[18] K. Eder *et al.*, Phys. Rev. Lett. **79**, 4112 (1997).
[19] M. L. Yu and K. Mann, Phys. Rev. Lett. **57**, 1476 (1986).
[20] R. Souda *et al.*, Phys. Rev. B **45**, 14 358 (1992).